A Numerical model for predicting the fire resistance of reinforced concrete beams

by V.K.R Kodur[1] and M. Dwaikat[2]

Abstract

A numerical model, in the form of a computer program, for tracing the behavior of reinforced concrete (RC) beams exposed to fire is presented. The three stages associated with the numerical procedure for evaluating fire resistance of RC beams; namely, fire temperature calculation, thermal analysis and strength analysis, are explained. A simplified approach to account for spalling under fire conditions is incorporated into the model. The use of the computer program for tracing the response of RC beams from the initial pre-loading stage to collapse stage, due to the combined effect of fire and loading, is demonstrated. The validity of the numerical model is established by comparing the predictions from the computer program with results from full-scale fire resistance tests. Through the results of numerical study, it is shown that the type of failure criterion has significant influence on predicting the fire resistance of RC beams.

Keywords: Fire resistance, high temperature, high strength concrete, reinforced concrete beams, spalling, numerical model

1 *Civil and Env. Eng., Michigan State University, East Lansing, MI 48824-1126* E-mail: kodur@egr.msu.edu
2 *Ph.D. Student, Civil and Env. Eng., Michigan State University, East Lansing, MI 48824-1126*

1. Introduction

Reinforced concrete (RC) structural systems are quite frequently used in high-rise buildings and other built infrastructure due to a number of advantages they provide over other materials. When used in buildings, the provision of appropriate fire safety measures for structural members is an important aspect of design since fire represents one of the most severe environmental conditions to which structures may be subjected in their life time. The fire resistance of reinforced concrete members is generally established using prescriptive approaches which are based on either standard fire resistance tests or empirical calculation methods [1,2]. There have been some recent advances towards performance-based fire resistance design approach for RC structural members [3]. However, such methods are still limited in scope and do not cover all important factors in the performance-based fire resistance design approach.

There have been limited studies on evaluating the fire performance of RC beams (mostly fabricated with normal strength concrete (NSC)). Thus, much of the current knowledge on fire behavior of RC concrete beams is based on standard fire resistance tests on beams (fabricated from NSC) under standard fire scenarios. There have been limited research studies on evaluating the fire performance of RC beams under realistic (design) fire scenarios. Thus, there is need for reliable experimental data, mathematical models and design specifications for predicting the fire resistance of RC beams under design fire scenarios. Furthermore, there are many drawbacks in the current approach of evaluating fire resistance of RC members based on standard fire tests. This is because the fire resistance of concrete members is based on limited fire tests which are carried out on specimens of standard sizes, one load level (50 % of room temperature capacity) and standard fire exposure. Therefore, the current prescriptive approaches for evaluating fire resistance do not represent realistic fire, loading and restraint scenarios as encountered in practice.

In addition, the use of high strength concrete (HSC) is becoming more popular due to the improvements in structural performance such as high-strength and durability that it can provide

compared to conventional NSC. The wider use of HSC, with questionable performance under fire conditions (due to factors such as occurrence of fire induced spalling) [4-6] has created an urgent need for developing more advanced, innovative and cost-effective solutions. While there have been some experimental studies on HSC columns under standard fire scenarios, there has been limited research on HSC beams under fire scenarios [6,7]. Thus, there is a lack of experimental data, mathematical models or design specifications for predicting fire resistance of HSC beams.

This paper presents the development of a computer model for predicting the fire behavior of RC beams under realistic fire, loading and failure scenarios. The model is based on a macroscopic finite element approach and uses a series of moment curvature relationships for tracing the response of the beam in the entire range of behavior, from a linear elastic stage to the collapse stage under any given fire and loading scenarios. The model is verified against experimental data by comparing the predicted temperatures, deflections and fire resistance times with the measured ones from fire tests. Results from numerical study are presented to illustrate the effect of failure criterion on fire resistance of RC beams. While this model is developed specifically for simply supported beams, the model can easily be extended to other cases such as continuous beams.

2. Fire Resistance of RC Beams - State-of-the-Art

A review of literature indicates that limited fire resistance tests have been conducted on RC beams. The most notable are the fire tests carried out by Lin et al. [8] and by Dotreppe and Franssen [9]. Lin et al. [8] tested eleven 305 mm X 355 mm RC beams under ASTM E119 [10] standard fire exposure. Their study investigated the influence of a number of factors including beam continuity, moment redistribution and aggregate type on the behavior of RC beams under standard fire conditions. One of the tested beams was simply supported at both ends, while the remaining beams were overhanging at one or both ends. The applied loading on the cantilever was chosen to reflect the continuity effect in RC beams. This study concluded that the fire resistance of continuous beams is much higher than that of simply supported beams due to the

occurrence of redistribution of bending moment and shear forces in fire conditions. The second experimental study, reported by Dotreppe and Franssen [9], involved testing a simply supported RC beam of rectangular cross section under ISO 834 [11] fire exposure. The main objective of this fire resistance test was to assess the fire resistance rating of an RC beam. More details about the properties and fire test results of the tested beams are given in Section 5.

The above reported fire tests, which considered a limited number of parameters, generally followed standard fire conditions and no realistic (design) conditions, such as fire exposure, specimen size, loading and failure conditions, were considered.

A review of the literature also shows that there have been few numerical studies on fire behavior of RC beams. The analytical studies reported by Dotreppe and Franssen [9], and Ellingwood and Lin [12], have a number of limitations. Specifically, they were not validated in the whole range of behavior (from the time the fire starts until the collapse of the beam) and do not account for important factors such as fire exposure scenario, failure criterion, concrete strength and load level. Also, the above analytical studies focused only on the behavior of RC beams fabricated with NSC and may not be applied for HSC beams. This is because, in case of HSC, spalling under fire situations is to be accounted for.

Some researchers theorized spalling to be caused by the build-up of pore pressure during heating [4,5,13,14]. HSC is believed to be more susceptible to this pressure build-up because of its low permeability compared to NSC. The extremely high water vapor pressure, generated during exposure to fire, cannot escape due to the high density of HSC and this pressure often reaches the saturation vapor pressure. At 300°C, the pressure reaches about 8 MPa. Such internal pressures are often too high to be resisted by the HSC mix having a tensile strength of about 5 MPa [4]. Data from various studies show that predicting fire performance of HSC, in general, and spalling, in particular, is very complex since it is affected by a number of factors [4-6].

3. Material Behavior at Elevated Temperatures

Generally, all structural members lose their strength and stiffness when exposed to high temperatures as encountered in fire. To ensure safety of RC structural systems in the event of fire, concrete members are to be designed against fire. Such design requires the use of numerical models.

Concrete generally has good fire resistance properties. The temperature dependent properties that are important for establishing an understanding of the fire-response of RC structures include: thermal, mechanical and material specific properties such as spalling of concrete and critical temperature for reinforcing steel. These temperature dependent properties are available in codes such as Eurocode 2 [3] and in the ASCE manual [15]. The variation of thermal conductivity and heat capacity of concrete are shown in Fig. 1 as a function of temperature. Also, the stress-strain curves (as given in the ASCE manual [15]) for NSC at various temperatures are shown in Fig. 2. It can be seen from the figures that the properties of concrete vary significantly with temperature, with large decrease in strength (stress) once the temperature exceeds 500 °C.

As illustrated in Section 2, there is a lack of numerical models for predicting the fire response of RC beams. Thus, the model presented here will help to better understand the high temperature behavior of RC beams under various design scenarios. In addition, such models are critical for overcoming many of the questions raised with respect to fire induced spalling in some concrete such as HSC.

4. Numerical Model

4.1 General approach

The numerical model, proposed here, uses moment-curvature relationships to trace the response of an RC beam in the entire range of loading up to collapse under fire. The model considers the case of loading where the bending moment is the dominant action on the beam and the effect of both shear force and axial force is neglected. The RC beam is divided into a number of segments along its length (as shown in Fig. 3) and the mid-section of the segment is assumed to represent the behavior of the whole segment. At any time step, the temperatures due to fire exposure are

established and then a thermal analysis is carried out to determine temperatures in each segment. Following this, a moment curvature (M-κ) relationship is generated for each segment at various time steps. It has been well established that M-κ relationships appropriately represent the behaviour of a RC beam at ambient conditions. In the current model, such M-κ relationships are established as a function of time for all longitudinal segments in the beam and they are in turn used to trace the response of the beam under fire conditions. The M-κ relationships, at various time steps, are generated using the changing properties of constituent materials namely concrete and reinforcement. In this way, the material nonlinearity will be implicitly accounted for in the analysis.

Using the M-κ relationships, the load (moment) the beam can carry at a particular time step is evaluated. Also, the deflection of the beam at that time step can be calculated through a stiffness approach by evaluating average stiffness of the beam. The average stiffness of the beam is computed using segmental stiffness, which is estimated by means of known M-κ relationships. The moment carrying capacity decreases with time, and the beam is said to attain failure if thermal, strength or deflection limit states are exceeded. A flowchart showing the numerical procedure for fire resistance calculations is given in Fig. 4.

The temperatures and strength capacities for each segment, and computed deflections in the beam are used to evaluate failure of the beam at each time step. At every time step, each beam segment is checked against pre-determined failure criteria, which include thermal and structural considerations. The time increments continue until a certain point at which the thermal failure criterion is met or the capacity (or deflection) reaches its limit state. At this point, the beam is assumed to have failed. The time to reach this failure point is the fire resistance of the beam. The model generates various critical output parameters, such as temperatures, stresses, strains, deflections and moment capacities at various given fire exposure times.

At each time step, the numerical calculations are performed in four steps: namely, calculation of fire temperatures to which the beam is exposed, calculation of temperatures in the beam, generation of M-κ relationships for each beam segment, and calculation of resulting beam deflection and strength through nonlinear structural analysis. These four steps are discussed in the following sections:

4.1.1 Fire temperature

The fire temperatures is calculated by assuming that three sides of the beam are exposed to the heat of a fire, whose temperature follows that of the standard fire exposure such as ASTM E119 [10] or any other design fire scenario [16]. The time-temperature relationship for the ASTM E119 standard fire can be approximated by the following equation:

$$T_f = T_0 + 750\left(1 - \exp\left(-3.79553\sqrt{t_h}\right)\right) + 170.41\sqrt{t_h} \qquad [1]$$

Where: t_h = time (hours), T_0 = initial temperature (°C), and T_f = fire temperature (°C)

For design fires, the time-temperature relationship specified in the SFPE [16] is built in the model. Also, to simulate hydrocarbon fire scenarios, the time-temperature relationship specified in ASTM E1529 [17] is incorporated into the model.

4.1.2 Thermal analysis

The fire temperatures computed above are used to calculate the temperatures within the beam cross section of each segment using a finite element method. The cross-sectional area of each segment is subdivided into a number of elements and temperature rise at every element within the cross section of a beam segment is derived by establishing a heat balance for each element. Detailed equations for the calculation of segment temperatures are derived [18].

The temperature is assumed to be uniform along the length of the segment and thus the calculations are performed for a unit length of each segment. Steel reinforcement is not

specifically considered in the thermal analysis because it does not significantly influence the temperature distribution in the beam cross section [19]. Generally, beams are exposed to fire from three sides as shown in Fig. 5. However, the heat transfer model is capable of predicting the cross sectional temperature distribution for any type of boundary conditions. The governing equation for transient heat conduction in an isotropic material is given as:

$$k\nabla^2 T + Q = \rho c \frac{\partial T}{\partial t} \qquad [2]$$

Where: k = thermal conductivity, ρc = heat capacity, T = temperature, t = time, and Q = heat source.

The boundary conditions for the heat transfer analysis can be expressed as:

$$k\left(\frac{\partial T}{\partial y} n_y + \frac{\partial T}{\partial z} n_z\right) = -h_t \left(T - T_\infty\right) \qquad [3]$$

Where: h_t = heat transfer coefficient, T_∞ = fire or ambient temperature depending on the type of exposure, n_y and n_z = components of the vector normal to the boundary in the plane of the cross section.

Galerkin finite element formulation is applied to solve Eq. [2] and four-node rectangular elements are used. In this approach, the material property matrices and the equivalent nodal heat flux (stiffness matrix K_e, mass matrix M_e, and nodal heat flux F_e) are generated for each element [18]. Once the element matrices are computed, they are assembled into a system of differential equations which can be written as:

$$M\dot{T} + KT = F(t) \qquad [4]$$

Where: K = global stiffness matrix, M = global mass matrix, and F = equivalent nodal heat flux.

$\dot{T}$ = temperature derivative with respect to time.

A finite difference procedure (θ algorithm) in the time domain is used to solve Eq. [4]. Thus, the following equation can be obtained [18]:

$$(M + h\theta K)T_{n+1} = (M - h(1-\theta)K)T_n + h(\theta F_{n+1} + (1-\theta)F_n) \quad [5]$$

Where: h = time step, T_n and T_{n+1} = temperature at the beginning and the end of time step, respectively, F_n and F_{n+1} = equivalent nodal heat flux at the beginning and the end of time step, and θ = a constant between 0 and 1.

For unconditional stability of the numerical calculations, θ has to be greater than or equal to 0.5 [18]. By knowing the temperatures at ambient conditions, Eq. [5] can be applied to obtain the temperature-time history at the following time step, and this can be repeated for subsequent time steps. In each time step, an iterative process is required to solve Eq. [5] due to the nonlinearity of both material properties and boundary conditions.

4.1.3 Strength analysis

The third step is the strength analysis (generation of M-κ relationships) at the mid-section of the segment. The cross-sectional temperatures generated from thermal analysis are used as input to the strength analysis. For the strength analysis, the following assumptions are made:

- Plane sections before bending remain plane after bending.
- Tensile strength of concrete, at elevated temperatures, is considered in the model based on the reduction factors proposed in Eurocode 2 [3].
- There is no bond-slip between steel reinforcement and concrete. This assumption implies that the total strain in the reinforcement is equal to that of the concrete. The assumption is quite accurate for the compression zone of concrete where no crack occurs. On the contrary, cracks may occur in the tensile zone causing weakness in the bond between concrete and reinforcement, and resulting in a slipping of this reinforcement. However, over a length that includes several cracks (beam segment), the average strain in both the reinforcement and the concrete are approximately equal

- Concrete of strength higher than 70 MPa is considered to be HSC. For HSC, the concrete strength in each element is computed based on the extent of spalling in that element.

The strength calculations, at elevated temperatures, are carried out using the same rectangular network described above and shown in Fig. 5(b). The temperatures, deformations and stresses in each element are represented by those at the center of the element. The temperature at the center of the concrete element is obtained by averaging the temperatures of the nodes of that element in the network. The same procedure is used for steel reinforcement, with the values of stress, strain components and temperature of each bar are represented by those at the center of the bar. The temperature at the centre of a steel bar is approximated by the temperature at the location of the center of the bar cross section.

The total strain in a concrete element, at any fire exposure time, is given as the sum of the thermal expansion of the concrete, the mechanical strain, the creep strain, and the transient strain:

$$\varepsilon_t = \varepsilon_{th} + \varepsilon_{me} + \varepsilon_{cr} + \varepsilon_{tr} \qquad [6]$$

Where: ε_t = total strain, ε_{th} = thermal strain, ε_{me} = mechanical strain, ε_{cr} = creep strain, and ε_{tr} = transient strain.

Thermal strain is directly dependent on the temperature in the element and can be obtained by knowing the temperature and thermal expansion of the concrete. Thermal strain is calculated in the model by integrating the coefficient of thermal expansion (which depends on the temperature of concrete) over the temperature domain. Creep strain is assumed to be function of time, temperature and stress level, and is computed based on Harmathy's [20] approach using the following expression:

$$\varepsilon_{cr} = \beta_1 \frac{\sigma}{f_{c,T}} \sqrt{t}\; e^{d(T-293)} \qquad [7]$$

Where: $\beta_1 = 6.28\times10^{-6}$ s$^{-0.5}$, $d = 2.658\times10^{-3}$ K^{-1}, T = current concrete temperature (K), t = time (s), $f_{c,T}$ = concrete strength at temperature T, and σ = current stress in the concrete.

The transient strain, which is specific for concrete under fire conditions, is computed based on the relationship proposed by Anderberg and Thelandersson [21]. The transient strain is related to thermal strain as follows:

$$\Delta\varepsilon_{tr} = k_2 \frac{\sigma}{f_{c,20}} \Delta\varepsilon_{th} \quad [8]$$

Where: k_2 = a constant ranges between 1.8 and 2.35 (a value of 2 will be used in the analysis); $\Delta\varepsilon_{th}$ = change in thermal strain; $\Delta\varepsilon_{tr}$ = change in transient strain and $f_{c,20}$ = concrete strength at room temperature.

For steel reinforcement, the total strain, at any fire exposure time, is calculated as the sum of three components as given by the following equation:

$$\varepsilon_{ts} = \varepsilon_{ths} + \varepsilon_{mes} + \varepsilon_{crs} \quad [9]$$

Where: ε_{ts}, ε_{ths}, ε_{mes} and ε_{crs} are total strain, thermal strain, mechanical strain and creep strain in the steel reinforcement, respectively.

Similar to concrete, thermal strain in steel can be directly calculated from the knowledge of rebar temperature and thermal expansion of the reinforcing steel. Creep strain is computed based on Dorn's theory and the model proposed by Harmathy [22] with some modifications made to account for different values of yield strength of steel. According to Harmathy's model, creep strain in steel is given by the following expression:

$$\varepsilon_{crs} = \left(3Z\varepsilon_{t0}^2\right)^{1/3} \theta^{1/3} + Z\theta \quad [10]$$

Where:

$$Z = \begin{Bmatrix} 6.755\times10^{19}\left(\dfrac{\sigma}{f_y}\right)^{4.7} & \dfrac{\sigma}{f_y} \le \dfrac{5}{12} \\ 1.23\times10^{16}\left(e^{10.8\left(\sigma/f_y\right)}\right) & \dfrac{\sigma}{f_y} > \dfrac{5}{12} \end{Bmatrix},$$

$\theta = \int e^{-\Delta H/RT} dt$, $\frac{\Delta H}{R} = 38900°\text{K}$, t = time (hours), $\varepsilon_{t0} = 0.016\left(\frac{\sigma}{f_y}\right)^{1.75}$, σ = stress in steel,

and f_y = yield strength of steel.

Fig. 6 shows the distributions of total strain, stress and internal forces for the beam cross section at any fire exposure time. The total strain in any element (concrete or rebar) can be related to the curvature of the beam by the following expression:

$$\varepsilon_t = \varepsilon_c + \kappa y \qquad [11]$$

Where: ε_c = strain at the top most fiber in concrete, κ = curvature, and y = the distance from the uppermost fiber of the beam cross section.

In the model, Eq. [6] to Eq. [11] can be used to carry out strain computation of a segment at any given fire exposure time. At any time step, and for an assumed value of ε_c and κ, the total strain in each element (concrete or rebar) can be determined using Eq. [11]. Then the thermal, transient (for concrete only), and creep strains in the concrete and rebars are evaluated using known temperatures and corresponding equations derived above. Using the knowledge of total strain, and thermal, transient, and creep strains, the mechanical strain in the element can be expressed by rearranging Eqs. [6] and [9]:

$$\varepsilon_{me} = \varepsilon_t - \varepsilon_{th} - \varepsilon_{cr} - \varepsilon_{tr} \qquad \text{for concrete} \qquad [12]$$

$$\varepsilon_{mes} = \varepsilon_{ts} - \varepsilon_{ths} - \varepsilon_{crs} \qquad \text{for steel} \qquad [13]$$

Then for the estimated mechanical strain, the stress in the element can be established using stress strain relationships for steel and concrete. Once the stresses are known, the forces in the element (concrete or rebar) are computed. These forces are used to check force equilibrium for each value of assumed strain and curvature. This iterative procedure is repeated till equilibrium, compatibility and convergence criterion are satisfied. Once these conditions are satisfied, moment and curvature corresponding to that strain are computed to represent one point on the moment-

curvature curve. Through this approach, various points on the moment-curvature curve are generated for each time step.

4.1.4 Beam analysis

The fourth step in the numerical calculations is the nonlinear structural analysis of the beam. In this step, the moment-curvature relationships generated for various longitudinal segments in the beam are used to trace the response of the whole beam exposed to fire. At each time step, the deflection of the beam is evaluated through stiffness approach. The secant stiffness for each segment is determined from the moment-curvature relationships, based on the moment level reached in that particular segment.

To compute the deflection of the beam at any time step and for a given loading conditions, the stiffness matrix and the loading vector are computed for each longitudinal segment. Then they are assembled in the form of nonlinear global stiffness equation, which can be written as:

$$K_g \, \delta = P \qquad [14]$$

Where: K_g = global stiffness matrix, δ = nodal displacements, and P = equivalent nodal loads.

The obtained system of nonlinear stiffness equations is solved using the iterative procedure described by Campbell and Kodur [23] and the deflections of the beam are computed

Thus, for any given time step, the temperatures (in concrete and steel), moment capacity and curvatures, as well as deflection and rate of deflection of the beam are known for a given fire exposure. These output parameters are used to evaluate the failure of the beam at local (in each segment) and global (whole beam) levels.

The conventional approach of evaluating fire resistance is based on thermal and strength failure criteria as specified in ASTM E119 [10]. However, deflections and rate of deflections play a major role in defining failure of RC beams under fire conditions. This is because the integrity of the structural member can not be guaranteed with excessive deformations. Moreover, defining

fire resistance based on limiting deflection will help to facilitate the safety of fire fighters and also to safely evacuate occupants prior to structural collapse [24]. Thus, four sets of failure criterion (one thermal, one strength, and two deflection limit states), are incorporated into the model to define failure of the beam in fire conditions. The first and second failure criteria are taken from ASTM E119 [10], while the third and the fourth failure criteria are taken from BS 476 [25]. Accordingly, the failure in an RC beam is said to occur when:

1. The applied service load exceeds the strength of the beam.
2. The temperature in reinforcing steel (tension reinforcement) exceeds 593 °C.
3. The deflection of the beam exceeds $L/20$ at any fire exposure time.
4. The rate of deflection exceeds the limit given by the following expression:

$$\frac{L^2}{9000d}\ (\text{mm/min}) \qquad [20]$$

Where: L = length of the beam (mm), and d = effective depth of the beam (mm).

4.2 Spalling

Spalling of concrete is incorporated into the model through a simplified approach proposed by Kodur et al. [26]. This approach is based on some experimental studies and considers various material and structural parameters that influence spalling. According to their model, the extent of spalling in HSC (which refers to the magnitude of spalling that can be partial or full) can be computed based on the following guidelines:

- Spalling occurs when the temperatures in an element exceed 350 °C.
- Spalling is influenced by the stirrup configuration adopted for the beam as follows:
  - Spalling occurs throughout the cross-section when the stirrups are bent in a conventional pattern (no hooks).
  - Spalling occurs only outside the reinforcement cage when the stirrups are bent at 135° into the concrete core.

- No spalling occurs when polypropylene fibers are present in the concrete mix.
- No spalling occurs inside the reinforcement core when the stirrup spacing is 0.7 times the standard spacing.
- The extent of spalling depend on the following factors:
  - Type of aggregate: the extent of spalling is higher (100%) in the siliceous aggregate HSC than that for carbonate aggregate HSC (40%).
  - Presence of steel fibers in the concrete mix: the extent of spalling in HSC beams with steel fiber is about 50%.

In addition, it is assumed that spalling does not occur in RC beams fabricated with NSC. This assumption is based on a number of experimental studies on NSC columns and beams, where there was no significant spalling in fire tests [27-29].

4.3 Material properties

Two sets of concrete properties suggested by Eurocode 2 [3] and those given in the ASCE Manual [15] were incorporated in the model. Type of aggregate has influence on the fire performance of concrete and therefore constitutive models for both siliceous and carbonate aggregate concretes have been incorporate into the model. Relevant formulas for both the mechanical and thermal properties of concrete as a function of temperature are built into the model. For reinforcing steel, the mechanical properties (stress-strain-temperature relationships) that are given in the ASCE Manual [15] are incorporated into the model.

5. Validation of the Model

The validity of the computer program is established through a set of numerical studies on three RC beams. The first beam, Beam I, is analyzed to illustrate the usefulness of the program in tracing the fire response of a typical RC beam in the entire range of loading up to collapse under fire exposure. The second and third beams, selected from literature, were analyzed to compare

model predictions with fire test data. The beam, Beam I, is representative of typical RC beams used in buildings and is analyzed under ASTM E119 standard fire exposure from three sides. Details of the beam dimensions, material properties and load level are given in Table 1 and Fig. 7.

5.1 Analysis of typical RC beam

Results from the analysis are used to demonstrate the behavior of a typical RC beam under fire conditions. To illustrate the thermal predictions from the model, the temperature variation is plotted as a function of fire exposure time at various locations of the beam cross-section in Fig. 8. The temperature at various depths of concrete, as well as in rebars, increases with fire exposure time. As expected, the predicted temperature decreases with increasing distance from the fire exposed side. It can be seen that the unexposed side of the beam stays unaffected for the first 60 minutes of the fire exposure time. This is due to the low thermal conductivity and high thermal capacity of concrete which slows down heat penetration to the inner layers of concrete. Also, it can be seen in the figure that the temperatures in the corner rebar is higher than that for central rebar throughout fire exposure time. This trend is on expected lines and can be attributed to the fact that corner rebars are exposed to fire from two sides, while the central rebar is exposed to fire from the bottom face only.

The obtained moment-curvature curves for the beam are shown in Fig. 9 at various time steps. The figure clearly shows that the moment capacity of the beam decreases with increasing time of fire exposure (increasing time steps). This is due to the deterioration in the material strength and stiffness as a result of increased temperatures in concrete and steel. The figure also shows that ultimate curvature (curvature at collapse) increases with time of fire exposure. This is mainly due to degradation of the material strength and stiffness as well as the creep strain which becomes significant prior to failure.

The variations of moment capacity and deflection in the beam are shown in Fig. 10 as a function of fire exposure time. It can be noted that the predicted moment capacity of the beam at room

temperature (179.8 kN.m) is slightly higher than the calculated moment capacity (156.6 kN.m) based on ACI 318 [30]. This is because the program allows for strain hardening of steel reinforcement which is not accounted for in the design equations of ACI 318 [30]. Fig. 10 also shows significant reduction in the moment capacity with time of fire exposure. However, the rate of reduction in the moment capacity decreases with fire exposure time. This can be attributed to the lower increase in rebar temperature towards the end of fire exposure time (due to lower rate of increase in fire temperatures) as shown in Fig. 8. In addition, Fig. 10 shows an increase in the beam deflection prior to failure. This trend is on the expected lines and is mainly due to yielding of steel and creep strains that become predominant just before the collapse of the beam. This is in agreement with reported test results from fire tests, which clearly show significant increase in deflection at later stages of fire exposure [31].

At elevated temperatures, strain components other than the mechanical strain (thermal, creep and transient strains) have to be considered. To illustrate the variation of the four strain components in concrete under fire condition, the four strains are plotted as a function of fire exposure time for point A (see Fig. 7 for location of point A) in Fig. 11. All four strain components starts out in a narrow range and the magnitude of creep, thermal and transient strains increases slightly towards the later stages of fire exposure. However, the magnitude of the mechanical strain is the dominant strain component and significantly increases just prior to failure time. This is mainly due to significant decrease in the stiffness of the beam and also due to higher creep, part of which is accounted for in stress-strain relationships.

The fire resistance for Beam I was computed according to the four sets of failure criterion discussed in Section 4.3 and is tabulated in Table 1. The fire resistance values, predicted based on the rebar temperature and strength failure criteria, are approximately similar. However, changing the load ratio or the mechanical properties of the constituent materials can produce different fire resistance values for strength failure criteria. On the contrary, these changes do not affect the rebar-temperature failure criterion since it is independent of these factors. Based on the deflection

and rate of deflection failure criteria, the program predicts150 and 159 minutes as fire resistance, which is lower than that predicted for temperature and strength failure criteria. Thus, deflection failure criterion governs the failure of Beam I and results in fire resistance of 150 minutes for that beam. As explained earlier ASTM E119 does not specify deflection or rate of deflection failure criterion, which can be a governing factor in determining the fire resistance of RC beams.

The failure times obtained from the model are also compared with the fire resistance values, calculated based on ACI 216.1 specifications, in Table 1. It can be seen that the fire resistance for Beam I, predicted by ACI 216.1, is higher than that predicted by the program. This is because the prescriptive approach in ACI relates the fire resistance of RC beams to the concrete cover thickness and the width of the beam only, and does not take into consideration factors such as load ratio (LR) and concrete strength.

5.2 Analysis of test beams

The validity of the computer model was established by comparing predicted results from the model with the measured values from fire tests for beams tested by Lin et al. [8] and Dotereppe and Franssen [9]. The geometric and material properties of the tested beams used in the analysis are taken from the literature and are given in Table 1. The fire resistance of the two beams (designated as Beam II and Beam III, respectively) is calculated based on the four sets of failure criterion discussed in Section 4.3 and summarized in Table 1. Predicted results from the analysis are compared to measured values from fire tests in Figs. 12 to 15.

In Fig. 12, the calculated average temperatures in the rebars are compared with the measured values for Beam II reported by Lin et al. [8]. It can be noted that there is good agreement between the predicted and measured values in the entire range of fire exposure. The steep increase in rebar temperature in the early stages of fire exposure is due to the occurrence of high thermal gradient at the beginning of fire exposure time as a result of faster increase in fire temperature (see ASTM E119 fire curve in Fig. 12). A review of predicted temperatures in concrete at various depths

indicated that the model predictions follow the expected trend with lower temperatures at larger depths from fire exposed surface. However, the predicted concrete temperatures could not be compared with test data since the measured temperatures were not reported by Lin et al. [8]. Figure 13 shows predicted and measured mid-span deflections as a function of fire exposure time for Beam II. It can be seen that model predictions are in close agreement with the measured deflections, throughout the fire exposure time.

The fire resistance of this beam was evaluated based on four failure criteria and its values are given in Table 1. The measured fire resistance, for Beam II, is lower than that predicted by the program for all failure criteria. This is mainly because the test was terminated after 80 minutes of fire exposure and before the beam attained complete failure probably due to sever conditions experienced towards the final stages in fire tests. Thus, the fire resistance of this beam would have been slightly higher if the test was continued till the complete failure. In addition, the difference between measured and predicted fire resistance can be partially attributed to variation in the material properties incorporated in the model from those of the actual beam. As an illustration, the current high temperature material property relationships do not take into account the variation of strength, heating rate, and other factors. There variations, though marginal, will have some influence on the results from the analysis. The fire resistance predicted based on rebar temperature (110 minutes) is much lower than that for strength failure criterion (140 minutes). This is because the rebar temperature failure criteria is based on load level of 50% of the room temperature capacity of the beam, however, the load level on this beam is lower than 50% and this results in higher fire resistance from strength failure criterion. In addition, the model predicted lower fire resistance based on deflection and rate of deflection failure criteria probably because the span/depth ratio for Beam II is large when compared to that for Beam I. Overall, the predicted fire resistance from deflection failure criteria (102 minutes) is a reasonable estimate to the measured value in the fire test (when the test was terminated).

Figs. 14 and 15 show the comparison of rebar temperatures and deflections for beam, Beam III, tested by Dotreppe and Franssen [9]. The material properties of this beam were not well reported in the published paper and thus the material properties used in the analysis are based on input from investigators [32], and are given in Table 1. It is clear from Fig. 14 that the model predictions match closely with measured values of rebar temperature from fire test. The predicted and measured mid-span deflections for Beam III are compared in Fig. 15. It can be noted that the deflections from the model compare well with the measured values throughout the fire exposure time. The good agreement in deflections can be attributed to capturing all the components of strain (in the model) that occurred during fire exposure. The slight differences that appear at later stages of fire exposure are probably because the high rate of deflection, at later stages of fire tests, makes the measuring process very difficult, and also reduce the reliability of the measured deflections.

The fire resistance values, based on four failure criteria, are tabulated in Table 1. The deflection and rate of deflection criteria result in fire resistance of 123 and 115 minutes, respectively, while the rebar temperature and strength criteria predict fire resistance of 120 and 145 minutes, respectively.

6. Design Implications

The current approach of evaluating fire resistance through standard fire tests on full-scale RC beams is expensive, time consuming and has a number of drawbacks. An alternative approach is to use calculation methods for predicting the fire resistance. However, such calculation methods are not widely available at present. Further, the current provisions in codes and standards [1,2] for evaluating fire resistance are prescriptive and simplistic in nature and thus can not be applied for rational fire safety design under the performance-based codes.

The computer model, presented here, is capable of tracing the behavior of RC beams from the initial pre-fire stage to the collapse of the beam under realistic fire and loading scenarios. Using the program, a designer can arrive at desired fire resistance in an RC beam by varying different fire, material and structural parameters, such as fire scenario, load, concrete strength and span length. Thus, the use of this program will lead to an improvement in design that is not only economical but is also based on rational design principles. Further, it facilitates the integration of the fire resistance design with structural design

The computer program can be applied to conduct a series of parametric studies to study the influence of various parameters on the fire resistance of RC beams. Data from such parametric studies can be used to develop rational and cost-effective fire safety design guidelines for incorporation into codes and standards. Such studies are currently in progress at Michigan State University.

7. Conclusions

Based on the results of this study, the following conclusions can be drawn:

- There is limited information on the fire performance of reinforced concrete beams, especially under design fire and realistic loading scenarios.
- The moment-curvature based macroscopic finite element model, presented in this study, is capable of predicting the fire behavior of reinforced concrete beams, in the entire range: from pre-fire stage to collapse stage, with an accuracy that is adequate for practical purposes. Using the model the fire resistance of a reinforced concrete beam can be evaluated for any value of significant parameters such as beam length, type of aggregate, section dimensions, without the necessity of testing.
- The limiting criterion, used for determining failure of a reinforced concrete beam exposed to fire, has significant influence on the fire resistance values. The conventional

failure criterion such as limiting rebar temperature or strength consideration may not be conservative under some scenarios. The deflection and rate of deflection failure criterion should be considered in evaluating fire resistance of reinforced concrete beams.

Acknowledgments

The research, presented in this paper, is primarily supported by the Michigan State University, through the Intramural Research Grant Program Award (IRGP 91-1452).

Reference

1. ACI Committee 216.1. Standard Method for Determining Fire Resistance of Concrete and Masonry Construction Assemblies. American Concrete Institute, Detroit; 1997.
2. ASCE/SFPE29. Standard Calculation Method for Structural Fire Protection. American Society of Civil Engineers, Reston, VA; 1999.
3. EN1992-1-2. Eurocode 2: Design of Concrete Structures. Part 1-2: General Rules - Structural Fire Design. Commission of European Communities, Brussels; 2004.
4. Diederichs U., Jumppanen U.M., Schneider U. High Temperature Properties and Spalling Behavior of High Strength Concrete. Proceedings of Fourth Weimar Workshop on High Performance Concrete, HAB Weimar, Germany; 1995. p. 219-235.
5. Kodur V.R. Spalling in High Strength Concrete Exposed to Fire - Concerns, Causes, Critical parameters and Cures. Proceedings: ASCE Structures Congress, Philadelphia, U.S.A; 2000. p. 1-8.
6. Kodur V.R. Guidelines for Fire Resistance Design of High Strength Concrete Columns. Journal of Fire Protection Engineering. Vol. 15, No. 2; 2005. p. 93-106.

7. Kodur V.R., Phan L. Factors Governing the Fire Performance of High Strength Concrete Systems. Proceedings: Fourth International Workshop - Structures in Fire; 2006. p. 573-585.
8. Lin T.D., Gustaferoo A.H., Abrams M.S. Fire Endurance of Continuous Reinforced Concrete Beams. PCA R&D Bulletin RD072.01B; 1981.
9. Dotreppe J.C., Franssen J.M. The Use of Numerical Models for the Fire Analysis of Reinforced Concrete and Composite Structures. Engineering Analysis, CML Publications. Vol. 2, No. 2; 1985. p. 67-74.
10. ASTM. Standard Methods of Fire Test of Building Construction and Materials. Test Method E119-01, American Society for Testing and Materials, West Conshohocken, PA, 2001.
11. ISO 834-1975. Fire resistance tests – elements of building construction. International Organization for Standardization; 1975.
12. Ellingwood B., Lin T.D. Flexure and Shear Behavior of Concrete Beams During Fire. Journal of Structural Engineering, ASCE. Vol. 117, No. 2; 1991. p. 440-458.
13. Kalifa, P., Menneteau, F.D., Quenard, D. (2000), "Spalling and pore pressure in HPC at high temperature", Cement and Concrete Research, 30 (12), pp. 1915-1927.
14. Bazïant, Z. P. (1997), "Analysis of pore pressure, thermal stress and fracture in rapidly heated concrete", Proceedings of International Workshop on Fire Performance of High-Strength Concrete, NIST, Gaithersburg, MD, pp. 155-164.
15. Lie T.T. (Editor). Structural Fire Protection. ASCE Manuals and Reports of Engineering Practice, No 78. American Society of Civil Engineers, New York; 1992.
16. SFPE. Fire Exposures to Structural Elements - Engineering Guide. Society of Fire Protection Engineers, Bethesda, MD; 2004. pp. 150.

17. ASTM. Standard Test Methods for Determining Effects of Large Hydrocarbon Pool Fires on Structural Members and Assemblies. Test Method E1529, American Society for Testing and Materials, West Conshohocken, PA; 1993.
18. William B.B. A first Course in the Finite Element Method. Richard D. Irwin, INC., US; 1990.
19. Lie T.T., Irwin R.J. Method to Calculate the Fire Resistance of Reinforced Concrete Columns with Rectangular Cross Section. ACI Structural Journal. American Concrete Institute. Vol. 90, No. 1; 1993. p. 52-60.
20. Harmathy T.Z. Fire Safety Design and Concrete. Concrete Design and Construction Series, Longman Scientific and Technical, UK; 1993.
21. Anderberg Y., and Thelandersson S. Stress and Deformation Characteristics of Concrete at High Temperatures, 2. Experimental Investigation and Material Behaviour Model. Lund Institute of Technology, Sweden; 1976.
22. Harmathy T.Z. A comprehensive Creep Model. Journal of Basic Engineering, Vol. 89, No. 2; 1967. p. 496-502.
23. Campbell T.I., Kodur V.K.R. Deformation Controlled Nonlinear Analysis of Prestressed Concrete Continuous Beams. PCI Journal, PCI; 1990. p. 42 – 55.
24. Kodur V.R., Dwaikat M.B. Performance-Based Fire Safety Design of Reinforced Concrete Beams. Journal of Fire Protection Engineering; 2007. p. 1-22.
25. BS. Fire Tests on Building Materials and Structures – Part 20: Method fro Determination of the Fire Resistance of Elements of Construction (General Principles). BS 476-3:1987, BSi, UK; 1987.
26. Kodur V. K. R., Wang T., Cheng F. Predicting the Fire Resistance Behavior of High Strength Concrete Columns. Cement & Concrete Composites, Elsevier Ltd. Vol. 26, No. 2; 2004. p. 141-153.

27. Aldea C.M., Franssen J.M., Dotreppe J.C. Fire Tests on Normal and High-Strength Reinforced Concrete Columns. International Workshop on Fire Performance of High-Strength Concrete, NIST, Gaithersburg, MD; 1997. P. 109-124.
28. Benmarce A., Guenfoud M. Experimental behaviour of high-strength concrete columns in fire. Magazine of Concrete Research, Vol. 57, No. 5; June 2005. , p. 283–287.
29. Kodur V.K.R. Fire resistance design guidelines for high strength concrete columns. NRCC-46116 ASCE/SFPE Specialty Conference of Designing Structures for Fire and JFPE, Baltimore, MD.; 2003. pp. 1-11.
30. ACI. Building Code Requirements for Reinforced Concrete. ACI 318-02 and Commentary - ACI 318R-2002, American Concrete Institute, Detroit, MI; 2002.
31. Kodur V.R., McGrath R.C. Fire Endurance of High Strength Concrete Columns. Journal of Fire Technology. Vol. 39, No. 1; 2003. p. 73-87.
32. Franssen J.M. Personal Communication on Fire Test Results for Reinforced Concrete Beams; June 1st, 2006.

Notation

b = beam width

c = clear concrete cover

C_t = total compressive force

d = effective depth of the beam

F = equivalent nodal heat flux

$f_{c,20}$ = concrete strength at room temperature

$f_{c,T}$ = concrete strength at temperature T

F_e = nodal heat flux

F_n, F_{n+1} = equivalent nodal heat flux at the beginning and the end of time step

f_y = yield strength of steel

h = time step

h_c, h_f = heat transfer coefficient of the cold and fire side

k = thermal conductivity

K = global stiffness matrix

k_2 = a constant ranges between 1.8 and 2.35

K_e = element stiffness matrix

K_g = global stiffness matrix for strength analysis

L = length of the beam

L_s = length of the beam segment

M = global mass matrix

M_e = element mass matrix

N = vector of the shape functions

n_y and n_z = components of the vector normal to the boundary in the plane of the cross section.

P = equivalent nodal load

Q = heat source

s = distance along the boundary

t = time

T = temperature

T_0 = initial temperature

t_h = time (hours)

T_f = fire temperature

T_n and T_{n+1} = temperature at the beginning and the end of time step, respectively

T_t = total tensile force

T_∞ = fire or ambient temperature depending on the boundary Γ

$\dot{T}$ = temperature derivative with respect to time

w = applied distributed load

y = the distance from the uppermost fibers of the beam

Z = Zener-Hollomon parameter for creep strain

α = h_c or h_f depending on the boundary Γ

δ = nodal displacements

$\Delta\varepsilon_{th}$ = change in thermal strain

$\Delta\varepsilon_{tr}$ = change in transient strain

ε_c = strain at the top most fibers of concrete

ε_{cr}, ε_{me}, ε_t, ε_{th}, ε_{tr} = creep strain, mechanical strain, total strain, thermal strain, and transient strain

ε_{crs}, ε_{mes}, ε_{ths}, ε_{ts} = creep strain, mechanical strain, thermal strain and total strain in steel.

ε_{t0} = creep strain parameter

κ = curvature,

θ = temperature-compensated time

ρc = heat capacity

σ = current stress in concrete or steel.

Table 1- Properties and Results for RC Beams used in the Analysis

Property	**Beam I**	**Beam II**	**Beam III**
Description	typical RC beam	tested by Lin et al 1981	tested by Dotreppe and Franssen 1985
Cross Section	300 mm × 500 mm	305 mm × 355 mm	200 mm × 600 mm
Length (m)	6	6.1	6.5
Reinforcement	2 ϕ 14 mm top bars	2 ϕ 19 mm top bars	2 ϕ 12 mm top bars
	3 ϕ 20 mm bottom bars	4 ϕ 19 mm bottom bars	3 ϕ 22 mm bottom bars
f'_c (MPa)	30	30	15*
f_y (MPa)	400	435.8	300*
Loading ratio	0.5	0.42	0.263*
Applied total load (kN)	120	80	65
Concrete cover thickness (mm)	40	25 (bottom) 38 (side)	40
Aggregate type	Carbonate	Carbonate	Siliceous*
Fire resistance based on failure criterion:			
• Rebar temperature	180	110	120
• Strength	185	140	145
• Deflection (BS 476)	150	102	123
• Rate of deflection (BS 476)	159	105	115
Fire resistance based on ACI 216	226	180	154
Fire resistance as obtained in test	-----	80	120

* Values based on correspondence (Franssen 2006)

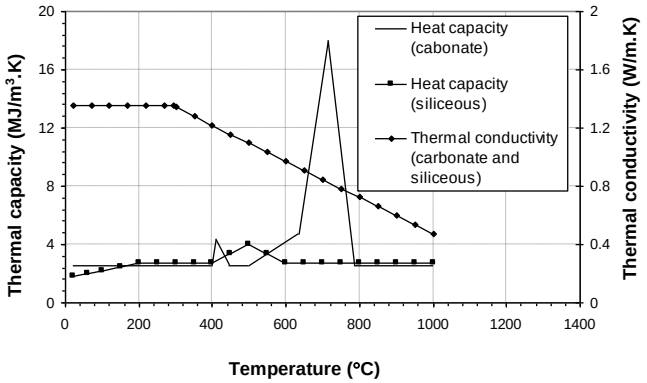

Fig. 1- Variation of thermal Properties of Concrete as a Function of Temperature [15]

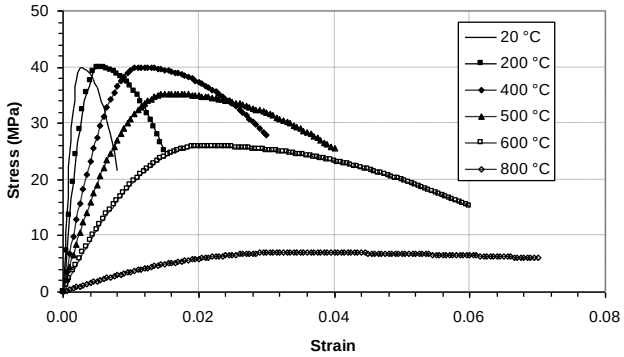

Fig. 2- Effect of temperature on stress-Strain Curves of Concrete (NSC) [15]

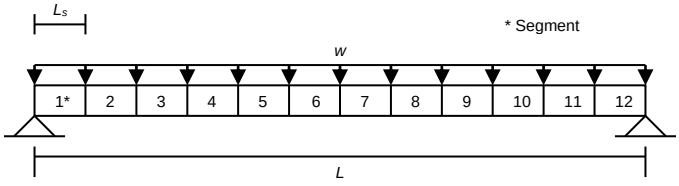

Fig. 3- Layout of a Typical RC Beam and its Idealization for Analysis

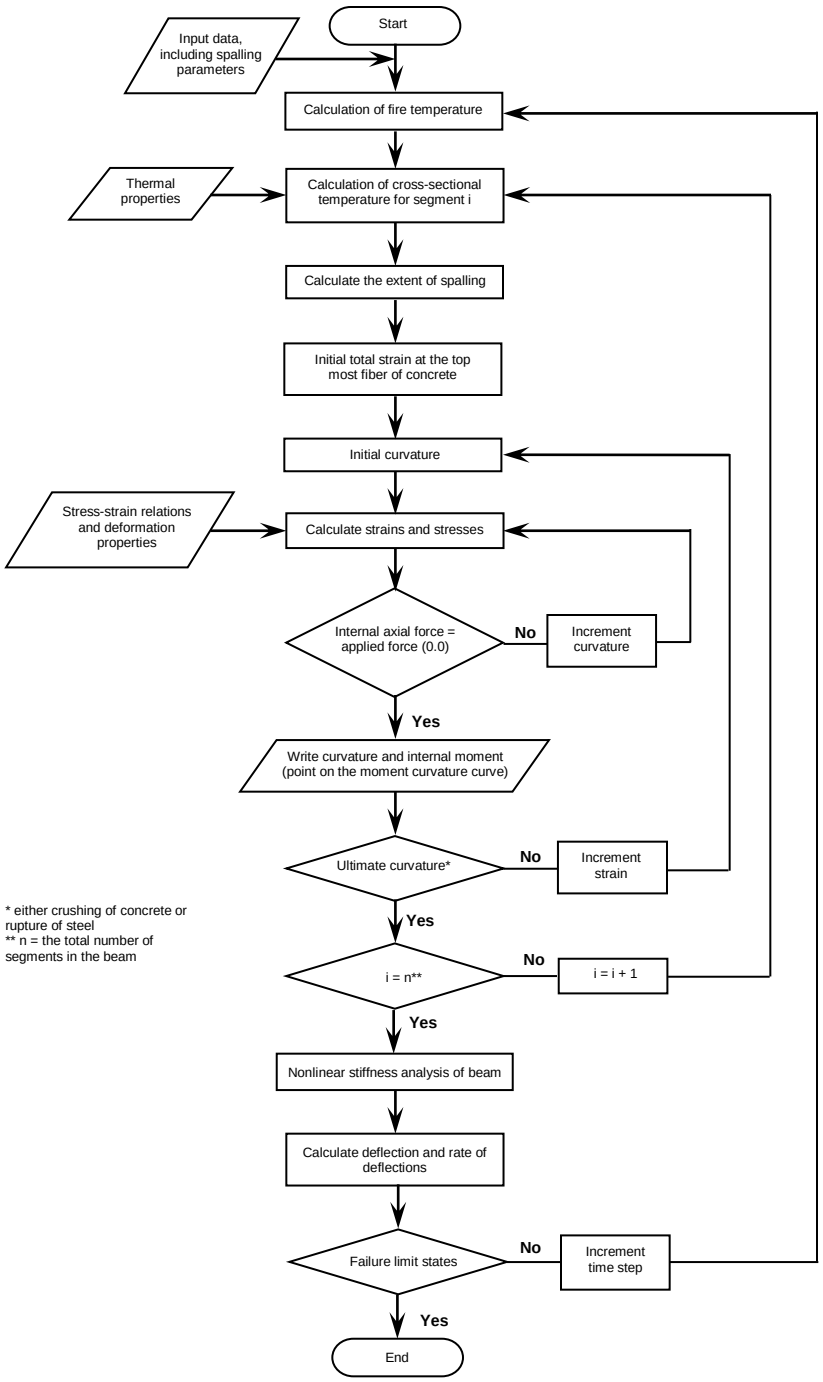

Fig. 4- Flowchart for the Analysis of RC Beams Exposed to Fire

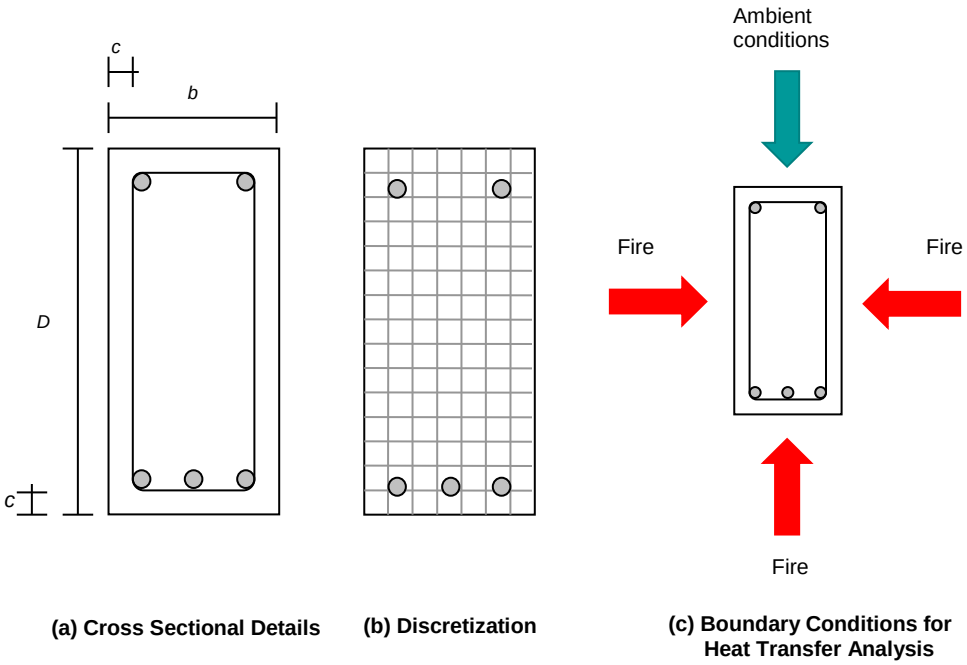

Fig. 5- Cross Section of an RC Beam and its Discretization for Analysis

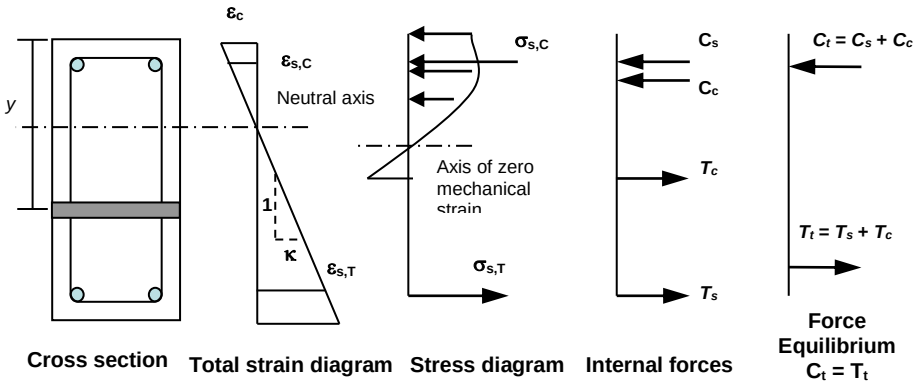

Fig. 6- Variation of Strain, Stress and Internal Forces in a Typical Beam Cross Section Exposed to Fire

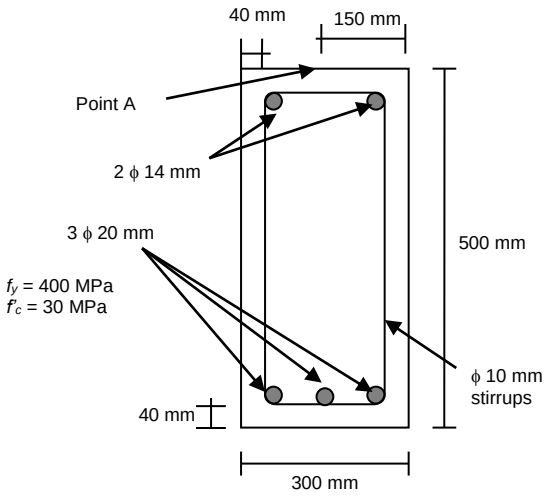

(b) Cross Section

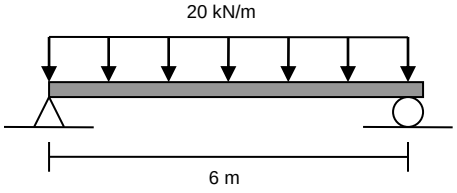

(a) Elevation

Fig. 7- Elevation and Cross Section of RC Beam, Beam I

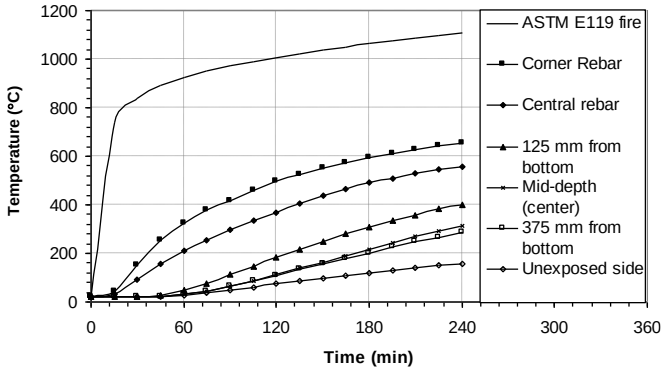

Fig. 8- Temperature as a Function of Time at different Locations of Cross Section in Beam I

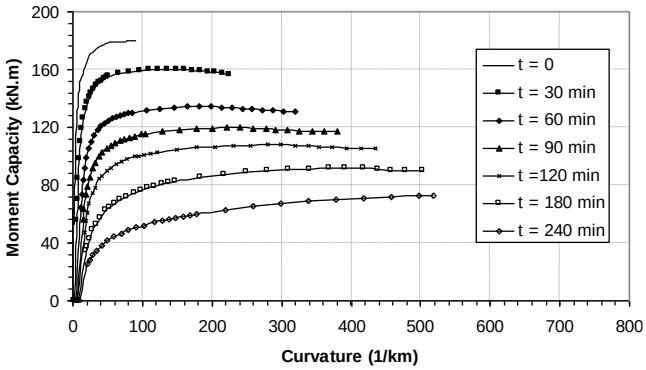

Fig. 9- Moment Curvature Curves at Various Times for Beam I under Fire Exposure

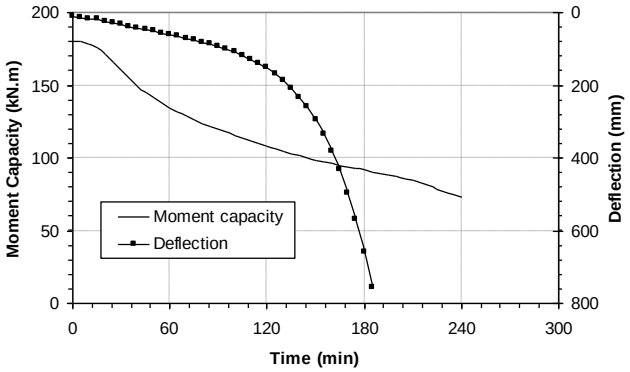

Fig. 10- Variation of Moment Capacity and Deflection for Beam I as a Function of Fire Exposure Time

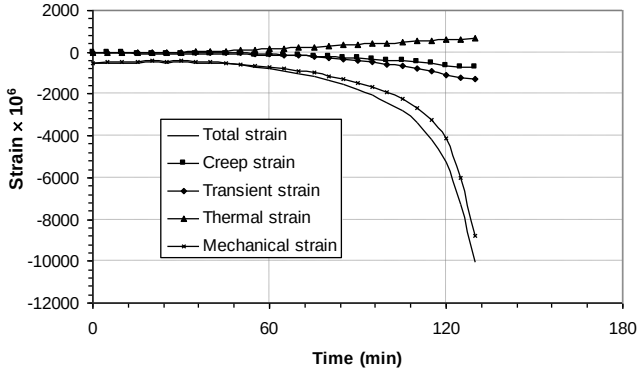

Fig. 11- Variation of Strain Components of Point A as a Function of Fire Exposure Time (see Fig. 7 for location of point A)

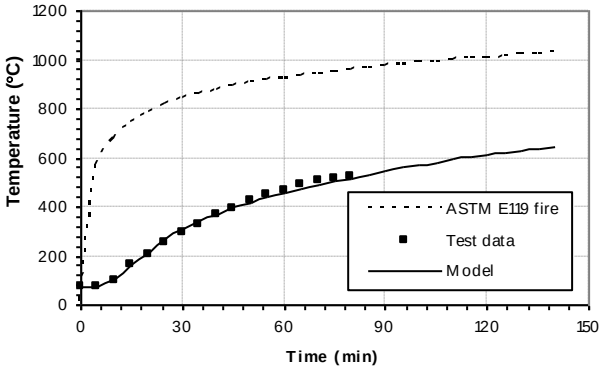

Fig. 12- Predicted and Measured Rebar Temperatures for Test Beam, Beam II

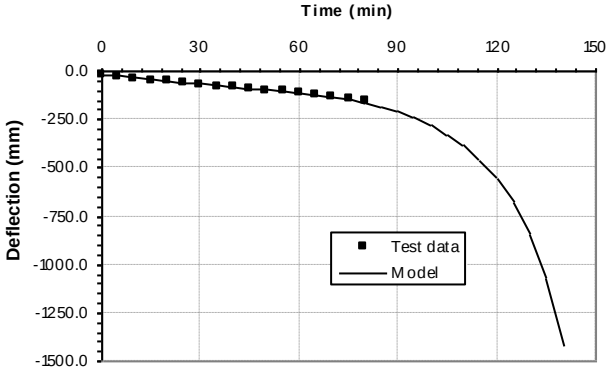

Fig. 13- Predicted and Measured Deflections for Test Beam, Beam II

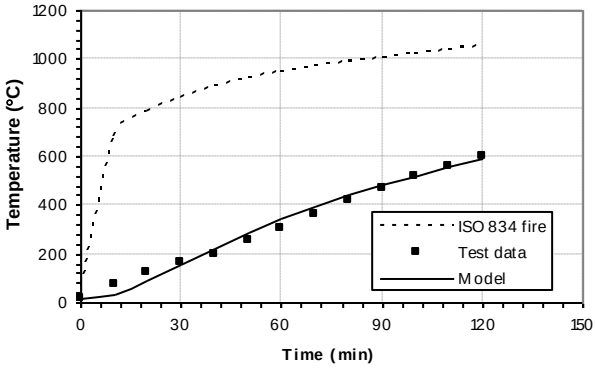

Fig. 14- Predicted and Measured Rebar Temperatures for Test Beam, Beam III

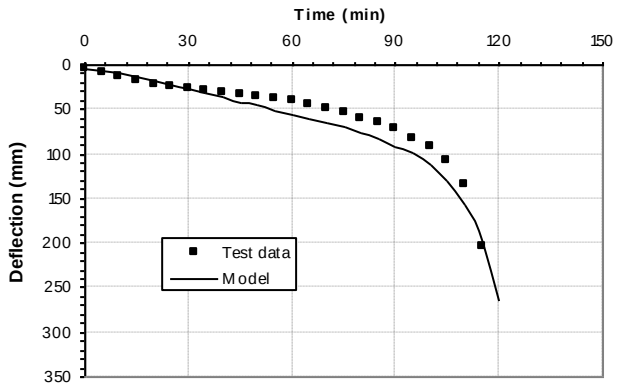

Fig. 15- Predicted and Measured Deflections for Test Beam, Beam III